CRITICAL PLANES CRITERIA APPLIED TO GEAR TEETH: WHICH ONE IS THE MOST APPROPRIATE TO CHARACTERIZE CRACK PROPAGATION?

FRANCO CONCLI & LORENZO MACCIONI
Faculty of Science and Technology, Free University of Bolzano, Italy

ABSTRACT

Tooth root bending fatigue is the most dangerous failure mode in gears. Indeed, it starts from the nucleation of a crack within the tooth root fillet region and the subsequent propagation up to the complete breakage of the tooth. To investigate this phenomenon, Single Tooth Bending Fatigue (STBF) tests are largely diffused. In these tests, an alternating bending stress at the tooth root is induced by the application of a pulsing force to the gear flank. In addition, this loading condition can be modelled through Finite Elements (FE) to study the stress state in the affected area. However, the application of strength criteria such as von Mises' can provide the equivalent stresses when the applied force reaches its maximum value but does not provide any insight in terms of fatigue behaviour. Nevertheless, the crack propagation can be investigated by analysing the results of FE analyses (which model the entire load cycle) through fatigue criteria based, for instance, on the critical plane concept. Previous studies conducted by the authors have shown that the different fatigue criteria (to study the tooth bending failure) lead to very different results. Therefore, the objective of the present paper is to compare the results of analyses carried out with different fatigue criteria based on critical plane, i.e. Findley, Matake, McDiarmid, Papadopoulos, and Susmel, with experimental outcomes, i.e. STBF tests on an aeronautical gears, to determine the most appropriate fatigue criterion to characterize the fatigue behaviour of these mechanical components. Results reveal that all fatigue criteria lead to consistent results when the target is to identify the most critical point. However, the Findley and Papadopulus criteria are found to be the most accurate for what concerns the evaluation of the damage. Among the others, Susmel turns out to be the most conservative criterion while the Findley criterion is the only one capable of identifying with good accuracy the direction of crack propagation.

Keywords: STBF, FEM, gears, fatigue, critical plane, crack.

1 INTRODUCTION

Nowadays, safety and reliability are undoubtedly Must-Be in the list of requirements for a gearbox and, therefore, the avoidance of failure due to the tooth root bending fatigue is a primary goal in gear design [1], [2]. With this respect, standards, e.g. ISO 6336-3 [3] and ANSI/AGMA [4], support gear design based on the determination of tooth bending strength. In particular, according to [3], the permissible bending stress is proportional to material strength that, in turn, is usually determined though experimental campaigns.

In the gear industry, the above-mentioned experimental campaigns are usually carried out by means of Single Tooth Bending Fatigue (STBF) tests [5]–[8] basically for economical and time reasons. In STBF tests, a gear made of the material and industrial processes to be tested is exploited as a specimen. Exploiting the Wildhaber property, two pulsating, competing, parallel and discordant forces are applied normal to two tooth flanks and tangent to the base circumference. In this way, using two simple anvils mounted on a universal testing machine, it is possible to load the teeth and to study the fatigue behavior experimentally [9], [10].

In order to study the stress state at the tooth root, experimental tests can be simulated numerically through Finite Element Models (FEM) [11], [12]. In this way, the force imposed by the anvils can be translated in terms of stresses in the studied area [13]–[15]. To improve this calibration process, strain gauges measurements can be exploited [16]. However, although the FEM results provide relevant information on principal stresses, to obtain additional information on fatigue behavior these data require further elaboration [17].

Recent studies conducted by the authors, revealed that the results of FEM simulations can be analyzed through fatigue criteria based on the critical plane. Through this approach, it is possible to assert the criticality of the various positions within the fillet at the tooth root and the potential direction of propagation of a crack. However, results show a strong dependency on the fatigue criterion used.

The aim of this paper is to compare experimental results with numerical ones to shed a light on which could be the most appropriate fatigue criterion to study tooth root bending fatigue. In particular, a STBF test carried out in [15], [16] has been simulated by means of FEM and the results have been analyzed with different fatigue criteria based on the critical plane concept, i.e. Findley [18], Matake [19], McDiarmid [20], Papadopoulos [21], and Susmel et al. [22]. The outcomes of the elaboration have been compared with images of the fractures that occurred in the experimental campaign described in [15], [16].

2 BACKGROUND

A general time dependent stress tensor, referred to a specific point, can be represented by eqn (1). The maximum octahedral stress $\sigma_{h,max}$ (in the time window T) can be calculated according to eqn (2), where $\boldsymbol{\sigma_O}$ is a vector containing the principal stresses that, for the same time instant t, satisfies eqn (3), where $\bar{\bar{\boldsymbol{I}}}$ is the identity matrix.

The stress vector $\boldsymbol{P_n}$ acting on a plane defined by a normal vector $\boldsymbol{n}(\phi_n, \theta_n)$ can be calculated through eqn (4). The modulus and the direction of $\boldsymbol{P_n}$ vary in time (Fig. 1(a)). In addition, $\boldsymbol{P_n}$ can be decomposed into a normal component $\boldsymbol{\sigma_n}$ (eqn (5)), having time-varying modulus and fixed direction, and a tangential component $\boldsymbol{\tau_n}$, having time-varying modulus and direction that, in turn, can be decomposed in its components aligned with the $\boldsymbol{u}$ and $\boldsymbol{v}$ directions respectively (eqn (6)) (Fig. 1(b)). $\boldsymbol{n}, \boldsymbol{u}, \boldsymbol{v}$ are defined as in eqn (7).

$$\bar{\bar{\boldsymbol{\sigma}}}(t) = \begin{bmatrix} \sigma_{xx}(t) & \tau_{xy}(t) & \tau_{xz}(t) \\ \tau_{yx}(t) & \sigma_{yy}(t) & \tau_{yz}(t) \\ \tau_{zx}(t) & \tau_{zy}(t) & \sigma_{zz}(t) \end{bmatrix} \tag{1}$$

$$\sigma_{h,max} = \max_T \left\{ \frac{1}{3} \sum_{i=1,2,3} \sigma_{O_i} \right\} \tag{2}$$

$$\det\left|\bar{\bar{\boldsymbol{\sigma}}}(\boldsymbol{t}) - \boldsymbol{\sigma_O} \bar{\bar{\boldsymbol{I}}}\right| = 0 \tag{3}$$

$$\boldsymbol{P_n}(\phi_n, \theta_n, t) = \bar{\bar{\boldsymbol{\sigma}}}(t)\, \boldsymbol{n}(\phi_n, \theta_n) \tag{4}$$

$$\boldsymbol{\sigma_n}(\phi_n, \theta_n, t) = \boldsymbol{n}^T(\phi_n, \theta_n) \bar{\bar{\boldsymbol{\sigma}}}(t)\, \boldsymbol{n}(\phi_n, \theta_n) \tag{5}$$

$$\boldsymbol{\tau_n}(\phi_n, \theta_n, t) = \boldsymbol{u}^T(\phi_n, \theta_n) \bar{\bar{\boldsymbol{\sigma}}}(t) \boldsymbol{u}(\phi_n, \theta_n) + \boldsymbol{v}^T(\phi_n, \theta_n) \bar{\bar{\boldsymbol{\sigma}}}(t)\, \boldsymbol{v}(\phi_n, \theta_n) \tag{6}$$

$$\boldsymbol{n}(\phi_n, \theta_n) = \begin{bmatrix} \cos\phi_n \sin\theta_n \\ \sin\phi_n \sin\theta_n \\ \cos\theta_n \end{bmatrix}; \boldsymbol{u}(\phi_n, \theta_n) = \begin{bmatrix} -\sin\theta_n \\ \cos\phi_n \\ 0 \end{bmatrix}; \boldsymbol{v}(\phi_n, \theta_n) = \begin{bmatrix} -\cos\phi_n \cos\theta_n \\ -\sin\phi_n \cos\theta_n \\ \sin\theta_n \end{bmatrix} \tag{7}$$

For periodic stresses, $\boldsymbol{P_n}$ describes a closed curve in the space and, therefore, $\boldsymbol{\tau_n}$ describes a closed curve in the plane. This curve is called as Γ_n in Fig. 1(b). With respect to $\boldsymbol{\sigma_n}$, along the period T, it assumes different values from a minimum $\sigma_{n,min}$ to a maximum $\sigma_{n,max}$ (Fig. 1(b)). Therefore, it is possible to define the value of the alternating stress (acting on the plane having normal $\boldsymbol{n}$) $\sigma_{n,a}$ according to eqn (8).

$$\sigma_{n,a} = \max_T\{\boldsymbol{\sigma_n}(t)\} - \min_T\{\boldsymbol{\sigma_n}(t)\} = \sigma_{n,max} - \sigma_{n,min} \tag{8}$$

The curve Γ_n is representative of the tangential stresses acting on the studied plane during the entire loading cycle. To translate Γ_n into a value of alternate tangential stress $\tau_{n,a}$ (exerting on the plane with normal $\boldsymbol{n}$) different methods can be found in the literature. The most diffused one is the Minimum Circumscribed Circle (MCC) (eqn (9)) [23], i.e. $\tau_{n,a}$ is considered as the radius of the smallest circle that can entirely contain the curve Γ_n (Fig. 2).

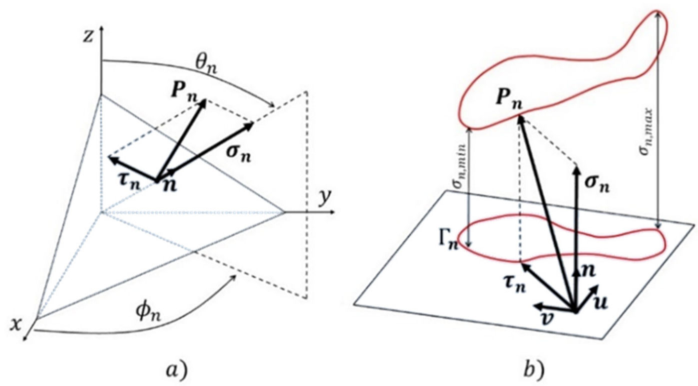

Figure 1: (a) Components of $\boldsymbol{P_n}(\phi_n, \theta_n, t)$ on the plane $\boldsymbol{n}(\phi_n, \theta_n)$; and (b) definition of the curve Γ_n.

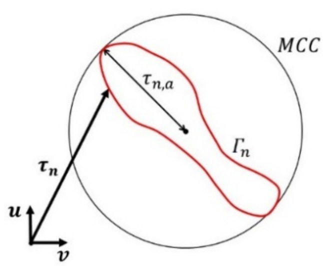

Figure 2: Minimum circumscribed circle (MCC) method.

$$\tau_{n,a} = \underset{T}{MCC}\{\boldsymbol{\tau_n}(t)\} \tag{9}$$

For each plane (having normal $\boldsymbol{n}$), that can be defined by varying the parameters (ϕ_n, θ_n), it is possible to compute the related stress parameters, i.e. $\tau_{n,a}$, $\sigma_{n,max}$, and $\sigma_{n,a}$. In the present paper, for the critical plane, the corresponding spherical coordinates and the related stresses will be labelled with the subscript c, i.e. $\phi_c, \theta_c, \tau_{c,a}, \sigma_{c,max}, and\ \sigma_{c,a}$.

The damage parameter of each fatigue criterion based on the critical plane can be represented as in eqn (10), where the parameters k and f are constants related to the material properties and S is a variable related to the normal stresses exerting on the critical plane. A summary on how the k, f and S parameters are defined based on the different fatigue criteria can be found in eqns (11)–(15). In particular, it is possible to notice that for the calculation of the parameter k according to the McDiarmid criterion, the ultimate tensile stress σ_R is required. For the other fatigue criteria, k can be calculated through the material fatigue limit at symmetrical alternating bending loading (σ_f), and the material fatigue limit at symmetrical alternating torsional loading (τ_f). With respect to the variable S, the Papadopoulos criterion considers the maximum octahedral stress $\sigma_{h,max}$ while, the others, consider stresses related to the critical plane, i.e. $\sigma_{c,max}$ in Finley and McDiarmid, $\sigma_{c,a}$ in Matake, and $\sigma_{c,max}/\tau_{c,a}$ in Susmel et al. [22]

$$DP = \tau_{c,a} + kS \leq f \tag{10}$$

$$DP_{Findley} = \tau_{c,a} + \frac{2r_{\tau/\sigma}-1}{2\left(\sqrt{r_{\tau/\sigma}-r_{\tau/\sigma}^2}\right)}\sigma_{c,max} \leq \frac{\tau_f}{2\left(\sqrt{r_{\tau/\sigma}-r_{\tau/\sigma}^2}\right)} \tag{11}$$

$$DP_{Matake} = \tau_{c,a} + \left(2r_{\tau/\sigma} - 1\right)\sigma_{c,a} \leq \tau_f \tag{12}$$

$$DP_{Susmel\ et\ al.} = \tau_{c,a} + \left(\tau_f - \frac{\sigma_f}{2}\right)\frac{\sigma_{c,max}}{\tau_{c,a}} \leq \tau_f \tag{13}$$

$$DP_{Papadopoulos} = \tau_{c,a} + \left(\frac{3}{2}\left(2r_{\tau/\sigma} - 1\right)\right)\sigma_{h,max} \leq \tau_f \tag{14}$$

$$DP_{\mathrm{McDiarmid}} = \tau_{c,a} + \frac{\tau_f}{2\sigma_R}\sigma_{c,max} \leq \tau_f \tag{15}$$

where

$$r_{\tau/\sigma} = \tau_f/\sigma_f \tag{16}$$

The determination of the critical plane (ϕ_c, θ_c) differs for the different fatigue criteria. According to the Findley criterion, the critical plane is the plane on which the damage parameter assumes its maximum value (eqn (17)) while, for the other fatigue criteria, the critical plane coincides with the one on which the $\tau_{c,a}$ reaches its maximum value (eqn (18)). Therefore, the application of the Findley criterion could lead to the identification of a critical plane having a different orientation with respect to the critical plane found applying the other fatigue criteria considered in this work. Eventually, the safety factor S_F can be defined as in eqn (19). $S_F > 1$ means that the analyzed point has not reached the critical value according to the studied criterion (and vice versa for $S_F < 1$).

$$(\phi_C, \theta_C) \to \max_{\phi,\theta}\left\{\tau_{n,a}(\phi,\theta) + kS(\phi,\theta)\right\} \tag{17}$$

$$(\phi_C, \theta_C) \to \max_{\phi,\theta}\left\{\tau_{n,a}(\phi,\theta)\right\} \tag{18}$$

$$S_F = \frac{f}{DP(\phi_C, \theta_C)} \tag{19}$$

3 MATERIAL AND METHOD

In the present paper, a gear geometry exploited in [22], [16] has been modelled in the STBF test condition. The gear parameters listed in Table 1 have been used as input in KISSsoft® to create a CAD model of the gear. Therefore, this model was imported into the open source FE software Salome-Meca/Code_Aster where the STBF test has been simulated.

Table 1: Geometrical parameter of the simulated gear.

Description	Symbol	Unit	Value
Normal module	m_n	(mm)	3.77301
Normal pressure angle	α_n	(°)	22.5
Number of teeth	z	(–)	32
Face width	b	(mm)	15
Profile shift coefficient	x	(–)	0.0681
Dedendum coefficient	h^*_{fP}	(–)	1.3153
Root radius factor	ρ^*_{fP}	(–)	0.36
Addendum coefficient	h^*_{aP}	(–)	1.1595

In the FEM simulation, symmetries were exploited to shorten the calculation time. In particular, a quarter of the gear has been meshed with an extruded grid. The quality of the mesh has been improved exclusively in the tooth subjected to the load. More specifically, the tooth in question have been meshed with hexahedral elements and the mesh density was increased in that region (Fig. 3). A non-linear simulation has been performed exploiting 40 time-steps (along the period T) for loading cycle. In Fig. 3, it is possible to see the faces in contact. The nodes of the anvil involved in the contact were 128 (105 hexahedral elements) while the nodes of the tooth flank involved in the contact were 248 (210 hexahedral elements). The radial symmetry (i.e. a plane containing the axis of the gear and parallel to the anvil contact face) was exploited to constrain the gear and a pulsating force varying sinusoidally from a minimum value of 3.7 kN to a maximum value of 37 kN was applied to the anvil to simulate the real testing condition. Indeed, this loading condition lead to the permissible bending stress for the studied gear according to [15], [16].

Typical steels properties have been applied to the components. The $\bar{\bar{\boldsymbol{\sigma}}}(t)$ in the nodes within the tooth root fillet region have been extracted (Fig. 3). In the present study, 31 nodes discretize the studied area, i.e. each point where fracture could nucleate. Moreover, the anvil has been modelled with 2,048 nodes (1,575 hexahedral elements), the contacting tooth has been modelled through 30,256 nodes (25,200 hexahedral elements) and the rest of the gear has been modelled through 15,230 nodes (19,296 tetrahedral elements). The above-mentioned mesh has been fine-tuned through a sensitivity analysis.

At this point, according with [24], the approaches presented in the background section have been applied to the results of the FEM simulation. In particular, the material studied presents $\sigma_f = 1{,}400\ MPa$, $\tau_f = 1{,}100\ MPa$, and $\sigma_R = 2{,}700\ MPa$. Consequently, the parameters k and f of eqn (10) can be calculated for each fatigue criteria according to eqns (11)–(15).

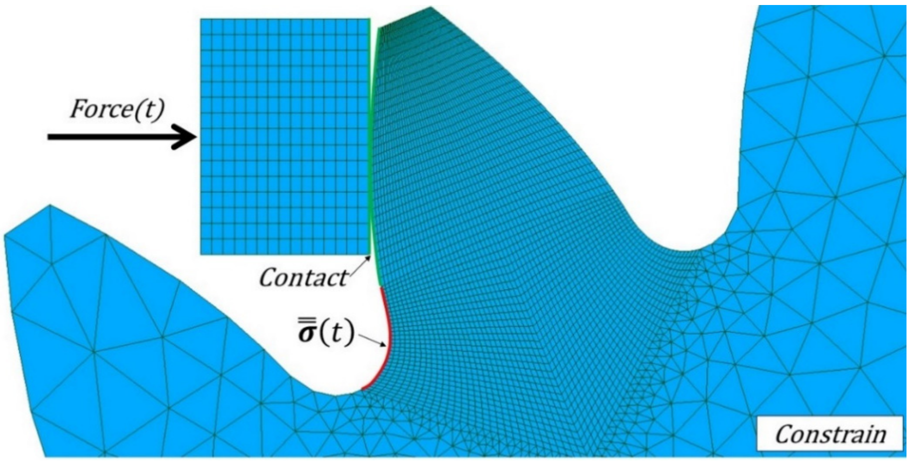

Figure 3: Finite element models of a STBF test.

Therefore, for each node within the tooth root fillet it is possible to study the stress tensor $\bar{\bar{\boldsymbol{\sigma}}}(t)$ through the fatigue criteria presented in the background section. In particular, it is possible to individuate the critical plane for each node N $(\theta_c \phi_c|_N)$. This can be performed through eqns (17) and (18). The identification of the critical plane for each node allows achieving a twofold objective. First, it allows to evaluate the damage parameter (through eqn (10)) and, therefore, to calculate S_F (eqn (19)). In this way, it is possible to recognize the most critical node and to evaluate the differences between the various nodes in terms of probability of failure. Second, it allows identifying the direction of the initial propagation of the crack if it nucleates in any of the studied nodes. The determination of this direction was used, in comparison with the experimental ones to assess the effectiveness of each criteria to correctly predict the failure. Indeed, in STBF specimens, it is possible to identify both the point where the crack nucleated and the direction of crack propagation for each tooth that failed for tooth bending fatigue during the test.

In the present study, $\bar{\bar{\boldsymbol{\sigma}}}(t)$ have been elaborated according to five different fatigue criteria i.e. Findley (eqn (11)), Matake (eqn (12)), Susmel et al. (eqn (13)), Papadopoulos (eqn (14)), and McDiarmid (eqn (15)). A Matlab routine have been implemented to explore all possible planes passing through each node with an angular resolution of 0.5° and identifying the critical planes. The results were compared with pictures of the STBF specimens to evaluate the capability of the various criteria to:

- identify the actual critical node;
- determine the actual crack direction; and
- provide a S_F consistent with the experimental measurements.

4 RESULTS AND DISCUSSION

A schematization of two cracks emerged during the experimental tests can be seen in Fig. 4. In particular, crack A is the recurrent one while crack B is nucleated in a different point probably due to the presence of defects in the material. This figure was created by observing the image of experimental specimens where the crack had broken the tooth or had propagated in its initial part. The actual images were not reported for confidentiality of the study. This schematization allows to:

- Identify the critical node, i.e. the intersection of crack A with the fillet; and
- Identify the direction of crack propagation at the critical node and at least one other node, e.g. crack B.

In Fig. 4, the angles between the direction of crack propagation and the tooth axis are shown. A coordinate χ that moves along the fillet has been defined. In Fig. 4, it is possible to see where this coordinate $\chi = 0$ and where $\chi = 1$ (values vary linearly along the profile of the fillet). Through this coordinate, it is possible to locate the critical node (e.g. $\chi = 0.40$ for crack A) and/or any point on the fillet at the tooth root (e.g. $\chi = 0.78$ for crack B). Such dimensions are obviously subject to measurement errors but are sufficiently accurate for the purposes of this paper.

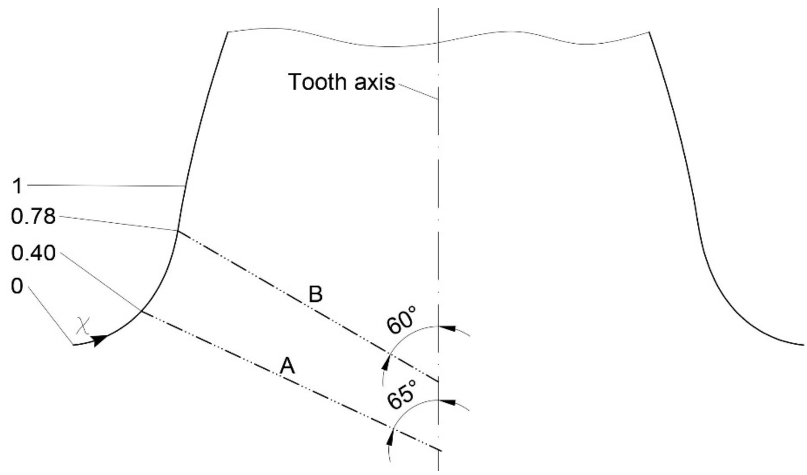

Figure 4: Schematization of experimentally detected cracks.

In Table 2, the S_F calculated according to different fatigue criteria are reported. In particular, the S_F has been calculated in the critical node, i.e. where the damage parameter is maximum (among the various nodes) for each criterion. More specifically, for the Findley and the Papadopoulos criteria the critical node is located at a coordinate $\chi = 0.39$ while for the other criteria the node $\chi = 0.42$. Therefore, it is possible to assert that all criteria identify the critical point with a variation less than 5%.

Table 2: S_F emerged through different fatigue criteria.

S_F according to				
Findley [18]	Matake [19]	Susmel et al. [22]	Papadopoulos [21]	McDiarmid [20]
1.08	1.96	0.79	1.13	2.14

Since the force set in the simulation leads to the permissible bending stress, S_F is expected to be equal to 1. Indeed, a lower force should lead to infinite life of the tooth (with the related induced stresses resulting below the fatigue limit). In Table 2, it is possible to notice that the criteria of Findley and Papadopoulos lead to S_F that approximate unitary values. Therefore, these fatigue criteria are the most appropriate to provide a S_F consistent with the experimental measurements. The Susmel et al. [22] criterion leads to the lowest S_F value and, therefore, it can be considered the most conservative one. The Matake [19] and McDiarmid [20] criteria lead to excessively high values of S_F and, therefore, they do not result to be appropriate to study tooth bending fatigue.

The graphical representation of the results according to the criteria of Findley and Papadopoulos are reported in Figs 5 and 6 respectively. This two-dimensional representation is made possible by the fact that all critical planes are perpendicular to the view shown. In the figures, the dash double-dotted segments represent the direction of the critical planes calculated for each node for the Findley (Fig. 5) and Papadopoulos (Fig. 6) criteria, i.e. the two criteria that provide more appropriate values of S_F. The length of each segment is proportional to the value of the damage parameter calculated on the relevant critical planes, i.e. the longest segment represents the plane on which the damage parameter is the maximum. The angle reported is exclusively for the critical plane passing through the critical node and the tooth axis. To simplify the identification of the critical plane having the highest damage parameter this has been made bold.

By comparing Figs 5 and 6, it is possible to notice how the Findley criterion leads to critical planes which form a greater angle with respect to the axis of the tooth e.g. 67° for the most critical plane. On the other hand, the Papadopoulos criterion, as well as the other criteria that identify the critical plane through eqn (18), lead to critical planes that tend to be less inclined with respect to the axis of the tooth e.g. 6° for the most critical plane.

In both Papadopoulos and Findley results, it is possible to observe a rapid variation in the angle of critical planes between some adjacent nodes. Applying Papadopoulos, this effect occurs at nodes near the origin of χ with a difference of about 85° between the two

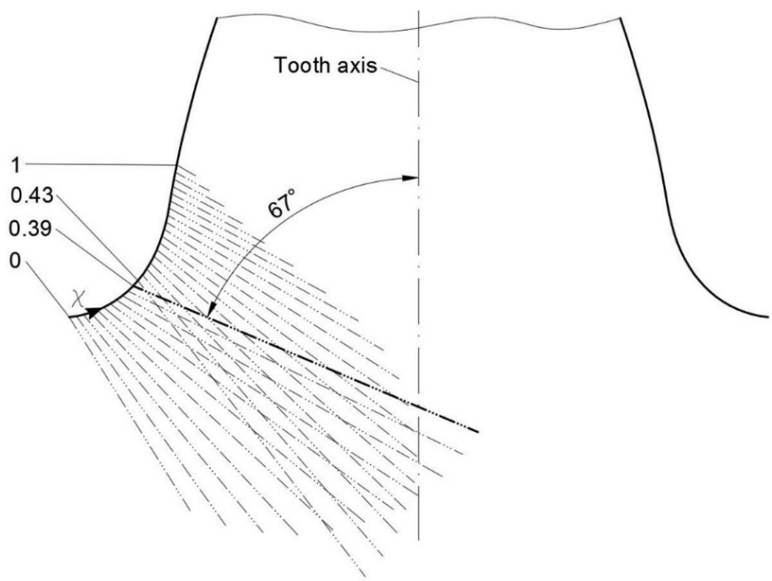

Figure 5: Critical planes passing through the various nodes within the tooth root fillet according to the criteria of Findley.

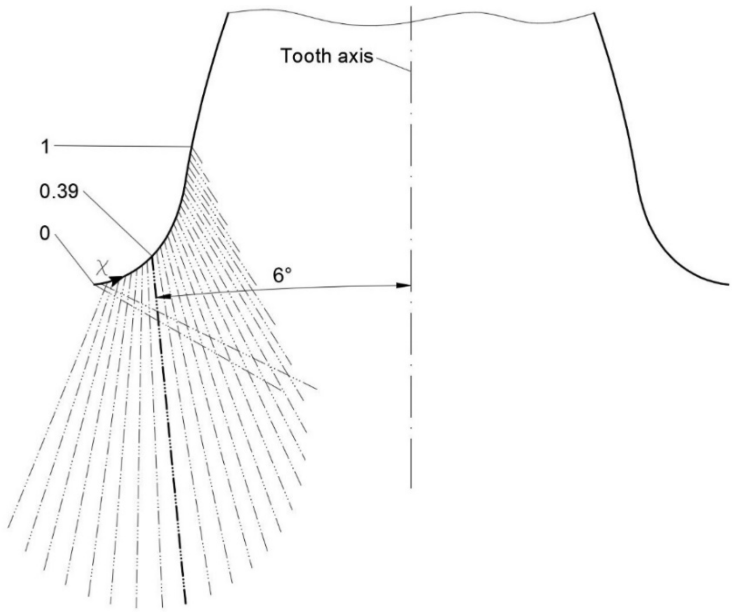

Figure 6: Critical planes passing through the various nodes within the tooth root fillet according to the criteria of Papadopoulos.

critical planes. On the other hand, applying Findley, it occurs between the two nodes having coordinates $\chi = 0.39$ and $\chi = 0.43$ with a difference of about 30° between the two critical planes. This phenomenon can be attributed to the notching effect of the fillet radius.

Eventually, by comparing the numerical results (Figs 5 and 6) with the experimental ones (Fig. 4) it clearly emerges that for both cracks (A and B in Fig. 4) the Findley criterion succeeds in better representing the direction of crack propagation. Indeed, crack A (Fig. 4) shows an angle of 65° and a critical point of coordinate $\chi = 0.40$ and it is well represented by the crack emerged by applying Findley in $\chi = 0.39$ which lead to a crack having an angle of 67°. The same can be observed for crack B (Fig. 4). Indeed, it shows an angle of 60° and a critical point of coordinate $\chi = 0.78$ and, in turn, it is well represented by the crack emerged by applying Findley in $\chi = 0.78$ that show an angle of around 58°.

The same comparison conducted exploiting the results of Papadopoulos and/or the other criteria, leads to errors even much greater than 45°.

5 CONCLUSIONS

In conclusion, criteria based on critical planes have been applied to the results of a FEM simulation (in terms of $\overline{\overline{\boldsymbol{\sigma}}}(t)$) to evaluate the damage of various points of the tooth root fillet due to fatigue and to identify the direction of crack propagation in case the crack nucleated near to ones of the studied points. More specifically, the simulation was set to represent an experimental condition studied in [15], [16] and the applied force was calibrated to achieve a permissible stress level i.e. a stress level that lead to a unitary safety factor. Images of cracks obtained experimentally were compared with numerical results achieved by applying the different fatigue criteria. The different fatigue criteria were compared according to their ability to (1) evaluate a factor of safety close to unity, (2) identify the critical point where usually the crack nucleates, and (3) identify the direction of crack propagation. Results reveal that Findley and Papadopoulos criteria lead to a S_F very close to unity in the most critical node i.e. 1.08 and 1.13 respectively. In addition, it has emerged that the criterion of Susmel et al. [22], is the most conservative leading to $S_F =$ 0.79 in the most stressed node. With respect to the individuation of the critical point, all the studied criteria reach the goal within a maximum variability of less than 5% of the arc length. Eventually, the fatigue criterion that better represents crack propagation is undoubtedly Findley's criterion.

Therefore, according to the results of this study, the Findley's criterion might be the most appropriate fatigue criterion for studying tooth bending fatigue. However, this statement is based on a single experimental validation conducted on a specific geometry and a specific material. Future studies conducted on different geometries and materials should be conducted to investigate the robustness of the insights obtained in this work.

REFERENCES

[1] Fernandes, P.J.L., Tooth bending fatigue failures in gears. *Engineering Failure Analysis*, **3**(3), pp. 219–225, 1996. DOI: 10.1016/1350-6307(96)00008-8.
[2] Hong, I.J., Kahraman, A. & Anderson, N., A rotating gear test methodology for evaluation of high-cycle tooth bending fatigue lives under fully reversed and fully released loading conditions. *International Journal of Fatigue*, **133**, p. 105432, 2020. DOI: 10.1016/j.ijfatigue.2019.105432.
[3] ISO 6336-3:2006, *Calculation of Load Capacity of Spur and Helical Gears, Part 3: Calculation of Tooth Bending Strength*, Standard: Geneva, CH, 2006.
[4] ANSI/AGMA 2001-D04, *Fundamental Rating Factors and Calculation Methods for Involute Spur and Helical Gear Teeth*, American Gear Manufacturers Association: Alexandria, 2004.
[5] Benedetti, M., Fontanari, V., Höhn, B.R., Oster, P. & Tobie, T., Influence of shot peening on bending tooth fatigue limit of case hardened gears. *International Journal of Fatigue*, **24**(11), pp. 1127–1136, 2002. DOI: 10.1016/S0142-1123(02)00034-8.
[6] McPherson, D.R. & Rao, S.B., Methodology for translating single-tooth bending fatigue data to be comparable to running gear data. *Gear Technology*, pp. 42–51, 2008.
[7] Dobler, D.I.A., Hergesell, I.M. & Stahl, I.K., Increased tooth bending strength and pitting load capacity of fine-module gears. *Gear Technology*, **33**(7), pp. 48–53, 2016.
[8] Concli, F., Tooth root bending strength of gears: Dimensional effect for small gears having a module below 5 mm. *Applied Science*, **11**, p. 2416, 2021. DOI: 10.3390/app11052416.
[9] Gorla, C., Conrado, E., Rosa, F. & Concli, F., Contact and bending fatigue behaviour of austempered ductile iron gears. *Proceedings of the Institution of Mechanical Engineers, Part C: Journal of Mechanical Engineering Science*, **232**(6), pp. 998–1008, 2018. DOI: 10.1177/0954406217695846.
[10] McPherson, D.R. & Rao, S.B., *Mechanical Testing of Gears*, ASM International: Materials Park, OH, pp. 861–872, 2000.
[11] Concli, F., Austempered ductile iron (ADI) for gears: Contact and bending fatigue behavior. *Procedia Structural Integrity*, **8**, pp. 14–23, 2018. DOI: 10.1016/j.prostr.2017.12.003.
[12] Bonaiti, L., Concli, F., Gorla, C. & Rosa, F., Bending fatigue behaviour of 17-4 PH gears produced via selective laser melting. *Procedia Structural Integrity*, **24**, pp. 764–774, 2019. DOI: 10.1016/j.prostr.2020.02.068.

[13] Gasparini, G., Mariani, U., Gorla, C., Filippini, M. & Rosa, F., Bending fatigue tests of helicopter case carburized gears: Influence of material, design and manufacturing parameters. *Fall Technical Meeting*, Vol. 369, ed. AGMA, American Gear Manufacturers Association (AGMA), pp. 131–142, 2008.
[14] Gorla, C., Rosa, F., Concli, F. & Albertini, H., Bending fatigue strength of innovative gear materials for wind turbines gearboxes: Effect of surface coatings. *ASME International Mechanical Engineering Congress and Exposition*, **45233**, pp. 3141–3147, 2012. DOI: 10.1115/IMECE2012-86513.
[15] Gorla, C., Rosa, F., Conrado, E. & Concli, F., Bending fatigue strength of case carburized and nitrided gear steels for aeronautical applications. *International Journal of Applied Engineering Research*, **12**(21), pp. 11306–11322, 2017.
[16] Gasparini, G., Mariani, U., Gorla, C., Filippini, M. & Rosa, F., Bending fatigue tests of helicopter case carburized gears: Influence of material, design and manufacturing parameters. *Gear Technology*, **68**, p. 76, Nov./Dec. 2009.
[17] Bonaiti, L., Bayoumi, A.B.M., Concli, F., Rosa, F. & Gorla, C., Gear root bending strength: A comparison between single tooth bending fatigue tests and meshing gears. *Journal of Mechanical Design*, pp. 1–17, 2021. DOI: 10.1115/1.4050560.
[18] Findley, W.N., A theory for the effect of mean stress on fatigue of metals under combined torsion and axial load or bending. *Journal of Engineering for Industry*, **81**(4), pp. 301–305, 1959. DOI: 10.1115/1.4008327.
[19] Matake, T., An explanation on fatigue limit under combined stress. *Bulletin of JSME*, **20**(141), pp. 257–263, 1977. DOI: 10.1299/jsme1958.20.257.
[20] McDiarmid, D.L., Fatigue under out-of-phase biaxial stresses of different frequencies. *Multiaxial Fatigue*, ASTM International, 1985. DOI: 10.1520/STP36245S.
[21] Papadopoulos, I., A high-cycle fatigue criterion applied in biaxial and triaxial out-of-phase stress conditions. *Fatigue & Fracture of Engineering Materials & Structures*, **18**(1), pp. 79–91, 1995. DOI: 10.1111/j.1460–2695.1995.tb00143.x.
[22] Susmel, L., Tovo, R. & Lazzarin, P., The mean stress effect on the high-cycle fatigue strength from a multiaxial fatigue point of view. *International Journal of Fatigue*, **27**(8), 928–943, 2005. DOI: 10.1016/j.ijfatigue.2004.11.012.
[23] Papadopoulos, I., Critical plane approaches in high-cycle fatigue: on the definition of the amplitude and mean value of the shear stress acting on the critical plane. *Fatigue & Fracture of Engineering Materials & Structures*, **21**(3), pp. 269–285, 1998. DOI: 10.1046/j.1460-2695.1998.00459.x.
[24] Concli, F., Fraccaroli, L. & Maccioni, L., Gear root bending strength: A new multiaxial approach to translate the results of single tooth bending fatigue tests to meshing gears. *Metals*, **11**(6), p. 863, 2021. DOI: 10.3390/met11060863.